The effects of special metallic dampers on the seismic behavior of a vulnerable RC frame

Hasan Özkaynak[*]

Department of Civil Engineering, Beykent University, Ayazaga 34396 Maslak, İstanbul, Turkey

Abstract. Earthquake excitations may induce important amount of seismic energy into structures. Current design philosophy mainly deals with the plastic deformations of replaceable energy dissipating devices rather than damages accumulated on structural members. Since earthquake damage is substantially concentrated on these devices they could be replaced after severe earthquakes. In this study, the efficiency of steel cushion (SC) on seismic improvement of a vulnerable reinforced concrete (RC) frame is determined by means of several numerical simulations. The cyclic shear behaviors of SCs were determined by performing quasi-static tests. The test results were the main basis of the theoretical model of SCs which were used in the numerical analysis. These analyses were performed on three types of RC frames namely *bare frame* (BF), *full-braced frame* (F-BF) and *semi-braced frame* (S-BF). According to analysis results; implementation of SCs has considerable effects in reducing the storey shear forces and storey drifts. Moreover plastic energy demands of structural elements were reduced which indicates a significant improvement in seismic behavior of the RC frame preventing damage accumulation on structural elements. Full-braced frame having SCs with the thickness of 25 mm has better performance than semi-braced frame interms of energy dissipation. However, global energy dissipation demand of S-BF and F-BF having SCs with the thickness of 18 mm are almost similar.

Keywords: metallic dampers; shear force; storey drift; energy dissipation; nonlinear time history analysis

1. Introduction

Global seismic behaviors of structures mainly depend on the performance of individual structural members such as columns and beams. Conventional forced based design principles concerns with the inelastic deformation capabilities of these members having unavoidable residual damages. However, recent earthquake design approaches are interested in the energy dissipation capacity of special devices. Among these devices, metallic dampers are evaluated as the most efficient ones to increase the structural performance without need of any complicated technology for their manufacturing and application. The energy dissipation in the metallic dampers simply occurs through the inelastic deformation of the metals. Implementation of metallic dampers to the structures can significantly decrease the inter storey drift and inelastic deformation demands of the primary structural members. Large portion of the earthquake input energy could be dissipated by these metallic dampers. There are numerous interests on the determination of cyclic behavior of metallic dampers in the recent literature. However, limited study highlights the efficiency of these devices on the seismic improvement of RC frames. The idea of absorbing the earthquake energy trough steel plates was first proposed by Kelly *et al*. (1972). According to the elementary tests, flat *U*

shaped steel elements could dissipate considerable amount of energy by rolling and bending. The metallic energy dissipative devices can be categorized into flexural types studied by Bergman and Goel (1987), triangular shape studied by Tsai *et al*. (1993); shear types studied by Chan *et al*. (2009) and axial types such as the buckling restrained braces studied by Black *et al*. (2004). Priestley (1991) studied energy dissipative steel elements in jointed wall system as special shear connectors in the content of Precast Seismic Structural Systems (PRESSS) program. Series of experiments were performed by Shultz and Magana (1996) to find out the flexural inelastic deformation capacity of the U-shaped plates (UFP). The UFP connector was proposed as flexible connectors which could be used as a source of plastic energy dissipation. Mazzolani (2007) performed full-scale experiments on real RC structures in order to investigate the performance of different metal based seismic upgrading techniques. Test results showed that the metal based innovative techniques, improved the original capacity of the RC structure in terms of strength, stiffness and ductility. Alehashem *et al*. (2008) performed numerical simulations on steel structures equipped with metallic dampers. They found out that the plastic deformations were accumulated on these metallic dampers by keeping the main structure safe. Oh *et al*. (2009) proposed a metallic slit damper to be used on beam-to-column connections. The test results showed that the energy dissipation and plastic deformation in the system were concentrated solely at the slit dampers. An experimental study was conducted by Sahoo and Rai (2010) on aluminum shear-yielding dampers which were installed in the steel jacketed RC frame.

---

[*]Corresponding author, Assistant Professor
 E-mail: hasanozkaynak@beykent.edu.tr

Significant increase in lateral strength, stiffness and energy dissipation capacity were achieved according to test results. The RC frame members did not suffer any major damage. This indicated significant reduction in force demand due to enhanced energy dissipation through hysteretic shear yielding of aluminum panels. Chan *et al.* (2009), performed cyclic tests on *steel slit damper* (SSD) which is a standard structural wide-flange section with a number of slits cut from the web. The test results showed that the device exhibited stable hysteresis with excellent energy dissipation and ductility. Gray *et al.* (2010), tested metallic elements which were implemented in concentrically braced frames. A stable symmetric inelastic response was achieved through the flexural yielding of metallic fingers. Experimental and analytical studies were performed by Maleki and Bagheri (2010) on cyclic behavior of steel pipes, filled and unfilled with concrete. The test results showed that the bare steel pipes are capable of absorbing a great amount of energy under severe cyclic shear loading with a stable hysteretic behavior. Karalis *et al.* (2011), conducted experimental and numerical works on RC frames. Steel I-shaped elements were implemented on the frames. The results showed that the use of the steel elements could increase the strength, stiffness, but mainly the energy dissipation capacity of the frame. Rai *et al.* (2013) conducted a shake table study on single-bay two-storey scaled concentrically braced frame specimen by using aluminum shear-links. Significant amount of energy was absorbed by the aluminum shear-links which acted as energy dissipation device. Valente (2013) performed numerical investigations on four-story RC frame with dissipative bracing system. Results of nonlinear dynamic analyses showed that the proposed bracing system can protect the primary structural elements and prevent them from damage under seismic actions. Zhang *et al.* (2015), proposed a simple and practical design methodology for retrofitting of earthquake-damaged frame structures by the use of metallic dampers.

In this study the efficiency of SCs on the seismic improvement of a vulnerable six-storey RC frame was evaluated in terms of storey drifts, storey/base shear forces and plastic energy dissipation demands. In order to achieve this, several *nonlinear-time history analyses* (NTHA) were performed on *bare frame* (BF) and the braced frames namely, *semi-braced frame* (S-BF) and *full-braced frame* (F-BF) under the affect of 13 earthquake records. Analysis results showed that, SC implementation exhibits a significant reduction in the plastic energy dissipation demand of structural members. Moreover SCs are effective to reduce the storey drifts and storey shear forces when compared with the bare frames. According to the analysis results, thickness of SCs and amount of braced frames are effective parameters in reducing both the base storey and upper storey drifts.

2. Analytical modeling

Quasi-static cyclic shear tests were carried out in order to determine the hysteretic behavior and energy dissipation capacity of SCs. A total of nine tests were performed on

SCs having three different thicknesses of 3, 5 and 8 mm. The analytical models of SCs mainly base on the experimental results.

2.1 Experimental background

Steel cushions are manufactured from mild steel through rolling a slice of steel plate and welding at one section. The rounding of steel sheets and welding are the essential stages of the manufacturing. Geometry of SC is composed of two main parts namely semi-circles and the straight parts. The geometry of SC is selected according to the numerical studies performed within the content of SafeCladding (2015). The cross-sectional dimensions of SCs are D=100 mm, *h*=250 mm and the plan width (b) is 100 mm, Fig. 1. The holes existing in the axis of symmetry is used for the connection.

The testing set-up is shown in Fig. 2. The testing protocol is based on the expected ultimate drifts selected according to FEMA461 (2007). According to the coupon tests, the yielding and ultimate strengths determined from the specimens were 350 MPa and 430 MPa respectively with the ultimate strain level of 20%. Steel cushions with
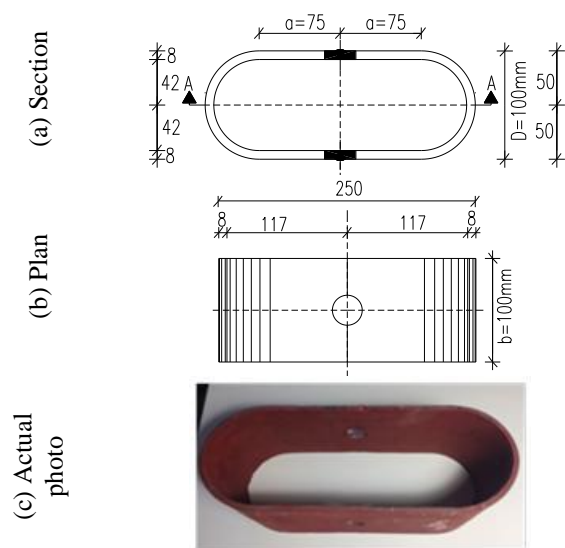

Fig. 1 Geometry of SC with the thickness of 8 mm
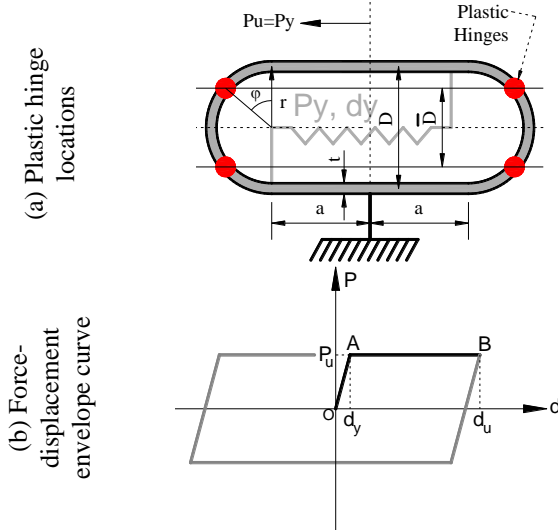

Fig. 2 Testing set-up

Fig. 3 Plastic hinge locations and the proposed backbone curve

Table 1 Calculated yielding parameters

t (mm)	f_{yd} (N/mm^2)	b (mm)	E (N/mm^2)	P_y (N)	d_y (mm)
3	350	100	200000	3351	7.6
5	350	100	200000	9210	4.51
8	350	100	200000	24348	2.91
18	350	100	200000	138293	1.45
25	350	100	200000	291667	1.14

the thickness of 8 mm had a nominal strength of 30 kN with a maximum displacement capacity of 220 mm. The nominal strengths of SCs with the thickness of 5 and 3 mm specimens are 10 kN and 3 kN, respectively. Great deformation capability and stable hysteretic curves are the common properties observed from the tested specimens. The cyclic shear tests of SCs showed that these elements have high energy dissipation capacity due to its special geometrical shape. All the other details regarding the experimental study could be found elsewhere in Ozkaynak *et al.* (2014).

2.2 Analytical modeling of SCs

Non-linear cyclic behavior of SCs is simulated by using a zero-length link element model pre-defined in SeismoStruct (2014) software program. The entire analytical model is composed of two stages. In the first stage bi-linear elasto-plastic force-displacement envelope curve is suggested, Fig. 3(b). The post-yield hardening ratio is neglected since it presented negligible values during the experiments.

The envelope curve is mainly defined with two important yielding parameters namely yield strength P_y ($=P_u$) and the yield displacement (d_y). These parameters were determined by the closed form equations for SCs as seen in Eqs. (1)-(4). The equations were extracted through the classical flexibility methods, SafeCladding (2015).

$$M_u = \frac{1}{4}\left(f_{yd}.b.t^2\right) \qquad (1)$$

$$P_y = 4Mu/D \qquad (2)$$

$$P_y = \frac{1}{D}\left(f_{yd}.b.t^2\right) \qquad (3)$$

$$d_y = \frac{P_u r^3}{4EI}\left(\frac{2\pi^2 a^2 + 8\pi ar + (3\pi^2 - 16)r^2}{2\pi a^2 + 8ar + \pi r^2}\right) \qquad (4)$$

The ultimate shear strength P_u ($=P_y$) could be calculated by the summation of the strengths of plastic hinges occurred at four critical points of SC, Fig. 3(a). The required parameters for predicting the ultimate shear strength (P_u) of SC are the yield strength of the material (f_{yd}), the width of SC (b), the thickness of the plate (t) and the height of SC (D). On the other hand, the parameters needed for prediction of the yield displacement (d_y), are the elasticity modulus of the material (E), the half-length of the unbended section (a), the radius of the bended section (r), and the moment of inertia of the section of cushion plate (I).

In the second stage of the analytical model, the envelope curve is fulfilled by *Ramberg-Osgood* hysteretic rules defined by Eq. (5) interms of P_y and d_y.

$$\frac{d}{d_y} = \frac{P}{P_y}\left(1 + \left|\frac{P}{P_y}\right|^{\gamma-1}\right) \qquad (5)$$

The yielding parameters P_y and d_y were calculated by the above closed form equations for varying thicknesses (t) and given in Table 1. It should be noted that the increment of thickness increases the strength and decreases the yield displacement. The yielding parameters shown in shaded rows are related with the SCs used for the numerical simulation study of the braced frames.

Force-displacement relations derived according to the analytical model for the selected case of SCs with the thickness of 3, 8, 18 and 25 mm are given in Fig. 4. The analytical results of SCs with the thickness of 3 and 8 mm are consistent with the experimental results. Divergence faced at large displacement levels was due to the contact of the bolt to the specimen during the experiment.

The cyclic shear tests performed on SCs and their analytical models showed that these elements have quite high energy dissipation capacity due to its special geometrical shape. Since they have enough energy dissipation capacity, they may be used as metallic dissipaters when they are placed in appropriate locations trough the structures.

2.3 Analytical modeling of bare and braced RC frames

A vulnerable six-storey and four-bay RC frame was selected for the numerical simulations. Each storey has the same height of 3.5 m. The total height of the frame is 21 m. In the lateral direction, the building includes four bays with the span length of 5 m. The braced frames are grouped into two types of bracing applications which are called as semi-braced frame (S-BF) and full-braced frame (F-BF). SCs
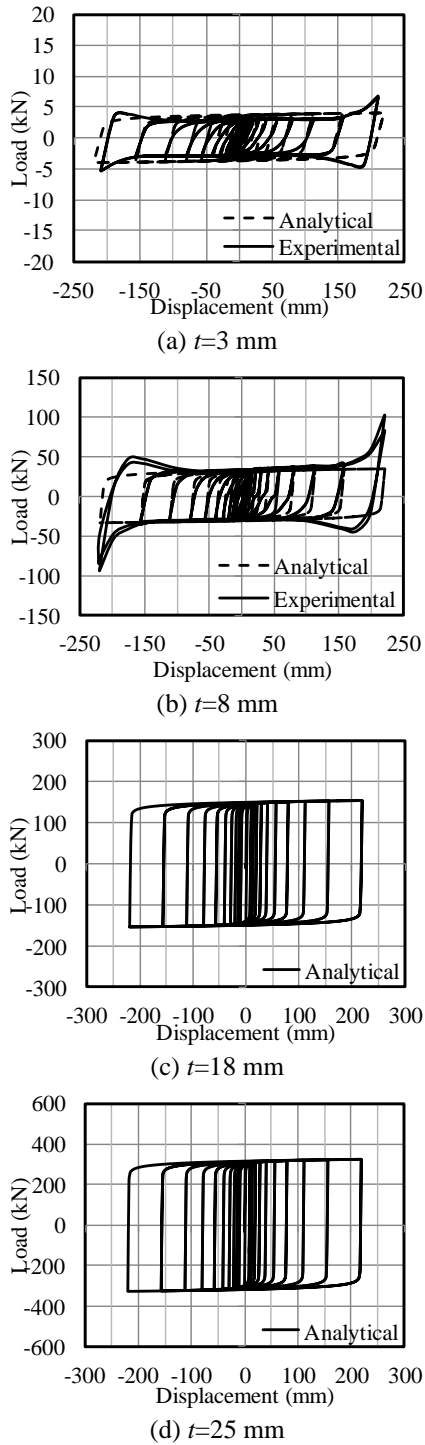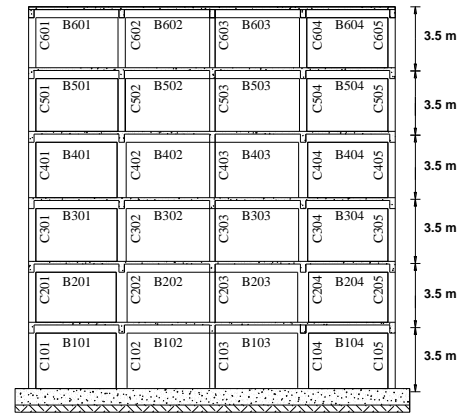
(a) *t*=3 mm

(b) *t*=8 mm

(c) *t*=18 mm

(d) *t*=25 mm

Fig. 4 Analytical models and experimental results

(a) Bare frame

(b) Semi-braced system and full-braced system

Fig. 5 Geometry of the RC structure

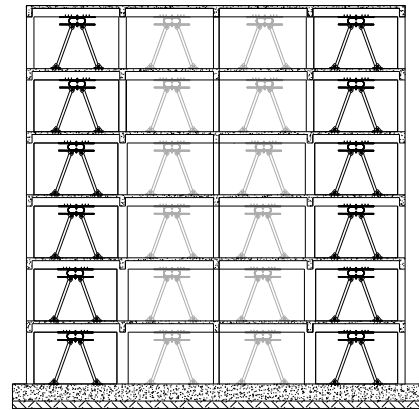Fig. 6 Implementation detail of SCs

were implemented in two edge bays throughout the height of the S-BF, where SCs were implemented in all bays of the F-BF. The schematic views of the bare and braced frames are illustrated in Fig. 5.

Schematic view of SC implementation to the RC frame is shown in Fig. 6. The analytical models of SCs with the thickness of 8, 18 and 25 mm given in Fig.4 were used during the numerical analysis of the braced frames (S-BF and F-BF).

Steel cushions were simply connected to the RC frame,
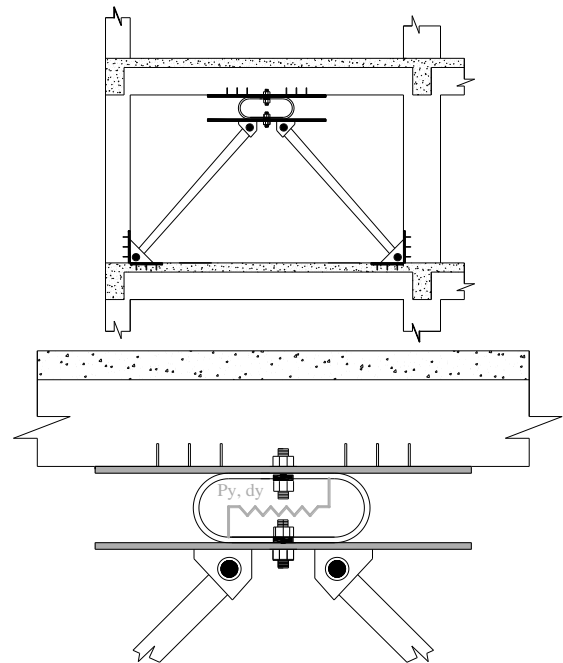
with pipe type bracing members which are 30 mm in diameter. The braces are defined as elastic elements having high axial rigidity. Since the braces remained elastic during the analysis, all the plastic deformations were condensed on

Table 2 Sectional dimensions and reinforcement configurations of column elements

Column#	b/h (cm)	Reinforcement
C101, C201, C301, C401, C501, C601, C105, C205, C305, C405, C505, C605	30/40	4Φ18 + 4Φ16
C102, C202, C104, C204	30/60	4Φ22 + 4Φ20
C302, C304, C402, C404	30/50	8Φ20
C502, C504, C602, C604	30/40	8Φ16
C103, C203	60/30	8Φ20
C303, C403	50/30	8Φ20
C503, C603	40/30	4Φ16 + 4Φ14

Table 3 Sectional dimensions and reinforcement configurations of beam elements

Beam#	b/h (cm)	Bottom re-bar	Top re-bar	Left support additional top reinforcement	Right support additional top reinforcement
B602, B502	30/60	3Φ16	2Φ12	2Φ18	2Φ14
B603, B503	30/60	3Φ16	2Φ12	2Φ14	2Φ18
B604, B501, B504, B601	30/60	3Φ16	2Φ12	2Φ18	2Φ18
B401, B404, B301, B304	30/60	4Φ16	2Φ14	3Φ20	3Φ20
B402, B302	30/60	4Φ16	2Φ14	3Φ20	2Φ20
B303, B403	30/60	4Φ16	2Φ14	2Φ20	3Φ20
B201, B101	30/60	4Φ16	3Φ14	2Φ22	3Φ22
B202, B102	30/60	4Φ16	3Φ14	3Φ22	1Φ22
B203, B103	30/60	4Φ16	3Φ14	1Φ22	3Φ22
B204, B104	30/60	4Φ16	3Φ14	3Φ22	2Φ22

Table 4 Summary of earthquake events for the far-field record set [FEMA P695]

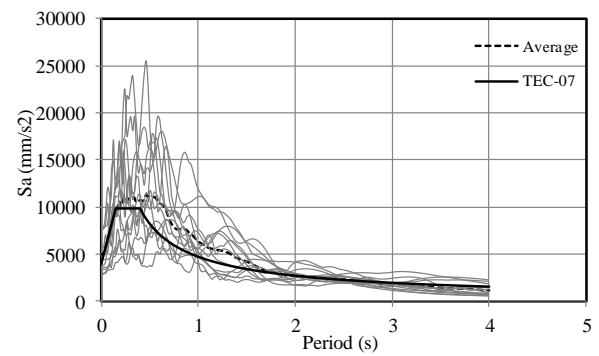| EQ ID	M	Year	Earthquake	EQ ID	M	Year	Earthquake
12011	6.7	1994	Northridge	12092	7.3	1992	Landers
12012	6.7	1994	Northridge	12101	6.9	1989	Loma Prieta
12041	7.1	1999	Duzce, Turkey	12102	6.9	1989	Loma Prieta
12052	7.1	1999	Hector Mine	12111	7.4	1990	Manjil, Iran
12061	6.5	1979	Imperial Valley	12121	6.5	1987	Superstition Hills
12062	6.5	1979	Imperial Valley	12122	6.5	1987	Superstition Hills
12071	6.9	1995	Kobe, Japan	12132	7.0	1992	Cape Mendocino
12072	6.9	1995	Kobe, Japan	12141	7.6	1999	Chi-Chi, Taiwan
12081	7.5	1999	Kocaeli, Turkey	12142	7.6	1999	Chi-Chi, Taiwan
12082	7.5	1999	Kocaeli, Turkey	12151	6.6	1971	San Fernando
12091	7.3	1992	Landers	12171	6.5	1976	Friuli, Italy

Fig. 7 Spectrum curves of far-field record set

the SCs. The pipes are attached to the beam column joints and to the SCs by a rotational hinge at both ends in order to prevent their flexural deformation and to enable the SC to deform in its lateral direction. Beam column joint regions were selected for the connecting point of bracing elements. At the top beam SC is directly bolted to the anchor which was embedded in the top beam concrete. Sectional dimensions and reinforcement configurations of the columns and the beams of the RC structure are given in Tables 2-3, respectively.

Strong axes of all the column elements of the frame are parallel in horizontal direction except the ones located in the symmetry axis. The RC slabs have infinite in plane rigidity and the thickness of slab is 15 cm. The structure includes regular frames with rigid connections. The frame elements are divided into mid-span and support regions to represent the confinement zones. The lateral reinforcements for the mid-span and confinement zone are distributed as Φ10/200 and Φ10/100 for the columns. The lateral reinforcements of the beams are Φ10/200 and Φ10/150 for the mid-span and confinement zone respectively. The theoretical model of the RC frame structure is created in Seismo-Struct (2014). Concentrated plasticity assumption is valid for the definition of the frame elements. However, the element types selected from the library are able to consider both geometric and material non-linearity throughout the

analysis. Confined concrete model is utilized for the definition of concrete material (Mander *et al*. 1988). The concrete compressive strength determined by means of cylindrical specimens extracted from the building is 18 MPa. The strains reached at the maximum stress and the strains at crushing stage were 0.002 and 0.004 respectively. All the RC members have 40 mm concrete cover. The behavior model for the reinforcement is bi-linear elasto-plastic material model having the same yielding strengths of 420 MPa for both lateral and longitudinal reinforcements. The yield and ultimate strains of the reinforcement is 0.002 and 0.008 respectively. The section analysis is performed within the Seismo-Struct (2014) program which takes into account the related dimensions and material properties.

Nonlinear time history analysis (NTHA) were performed by using 13 of 22 records of far-field record set which is selected by the methodology proposed in FEMA P695 (2009) and shown in Table 4 in shaded rows.

The original records were modified to attain an acceleration spectrum comparable with the descending branch of the target design spectrum defined in Turkish Earthquake Code (TEC2007). The structure is used as an office building and located on the firm type soil. The expected peak ground acceleration (PGA) is 0.4g for seismic Zone 1 and soil class Z2, Fig. 7. The code-based acceleration spectrum is 5% damped spectrum which has the corner points of T_a=0.15 sec and T_b=0.40 sec. Obtained acceleration records were used for the nonlinear time history analysis.

Table 5 Seismic weights of the RC structure

Storey #	1	2	3	4	5	6
Weight (kN)	793.38	796.60	787.73	782.01	772.25	480.87

Table 6 Maximum base storey drift ratio (%) observed for the bare and braced frames

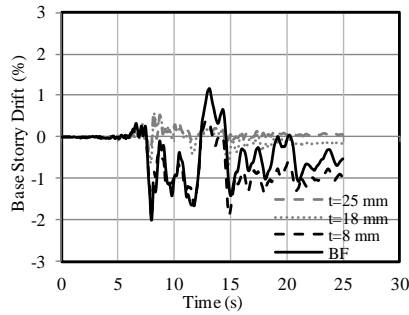| EQ#	BF	Semi- Braced Frame (S-BF)			Full- Braced Frame (F-BF)		
		$t=8$ mm	$t=18$ mm	$t=25$ mm	$t=8$ mm	$t=18$ mm	$t=25$ mm
12011	2.7	3.3	2.1	1.4	3.4	1.7	0.7
12012	2.3	2.3	1.8	1.5	2.0	1.9	0.9
12041	2.4	2.6	1.7	1	2.6	1.0	0.5
12061	1.9	1.3	1	0.7	1.1	0.7	0.4
12072	2.9	3.2	1.6	1	3.0	1.3	0.6
12081	2.0	1.9	0.7	0.5	1.7	0.5	0.4
12091	3.7	4.0	2	1.2	4.0	1.3	0.4
12121	3.1	2.8	1.8	1.4	2.3	1.6	0.5
12122	2.3	2.2	1.2	1	1.6	1.3	0.9
12132	2.0	2.1	2.2	2.0	2.5	2.5	1.0
12141	1.1	0.8	0.6	0.2	0.7	0.3	0.1
12142	3.3	3.5	1.9	1	3.4	0.8	0.2
12151	1.5	1.9	1.4	0.7	1.7	0.8	0.3
Average Drift Ratio (%)	2.4	2.4	1.5	*1.0*	2.3	*1.2*	*0.5*
Average Reduction (%)		~0.0	35.0	54	5.9	50.0	76.5

Table 7 Performance levels for primary elements of RC frames

Item	Collapse Prevention (CP)	Life Safety (LS)	Immediate Occupancy (IO)
Damage	Extensive cracking and hinge formation in ductile elements. Limited cracking and/or splice failure in some nonductile columns. Severe damage in short columns.	Extensive damage to beams. Spalling of cover and shear cracking < 3 mm for ductile columns. Minor spalling in nonductile columns. Joint cracks < 3 mm wide.	Minor hairline cracking. Limited yielding possible at a few locations. No crushing and strains < 0.003.
Drift (%)	4% transient or permanent	2% transient; 1% permanent	1% transient; negligible permanent

The seismic weights calculated for each storey according to TSE 498 (1997) is given in Table 5. According to free vibration analyses the fundamental period value amounting to 0.88 sec. was obtained for the case of bare frame, while the value of 0.67 sec and 0.40 sec corresponds to the *S-BF* and *F-BF* respectively. It should be noted that the fundamental period decreases with the increment of number of braced bays.

3. Seismic response results

A series of nonlinear dynamic time history analyses were conducted on *bare frame* (BF), and the braced frames namely, *semi-braced frame* (S-BF) and *full-braced frames* (F-BF) having SCs with the thickness of 8, 18 and 25 mm.

3.1 Base story and inter storey drifts

Maximum base storey drift values of bare frame and braced frames under the affect of 13 earthquake records are given in Table 6. Storey drift is defined as the ratio of storey displacement to the storey height. Base storey drift reduction ratio is calculated as the ratio of maximum base storey drift differences between bare and braced frame to the maximum base storey drift of the bare frame.

Storey drift is a crucial parameter to determine damage level and seismic performance level of a structure. Three performance levels of *immediate occupancy (*IO*), life safety*

(LS) and *collapse prevention* (CP) are defined interms storey drifts according to FEMA 356 (2000) and given in Table 7.

The average values of seismic analyses results confirmed that bare frame (BF) could neither achieve *immediate occupancy* (IO) nor *life safety* (LS) under the seismic actions of 13 earthquakes. A failure criterion of the frames during the analysis was assumed to be 4% storey drift. According to the numerical analyses, in most cases maximum base storey drift values of braced frames reduce when compared with the bare frames. In general, SC implementation is effective to reduce the average maximum base story drift values varying from 35% to 75% for different thickness and bracing systems. The average drift levels of S-BF and F-BF having SCs with thickness of 8 mm, were calculated as 2.4% and 2.3% respectively. Implementation of SCs with thickness of 8 mm was unsuccessful to improve the seismic performance of the bare frame interms of reducing base storey drifts. In the case of S-BF the averages of maximum base storey drift reduction ratios are 0.0%, 35.0% and 54.0% for the frames having SCs with the thickness of 8, 18 and 25 mm respectively. Average base storey drift reduction ratio of braced frames increases as the thicknesses of SCs increase. Thickness of SC is an efficient variable to decrease the base storey drifts. The average base storey drifts reduction ratios of S-BF having SC with the thickness of 25 mm was 54%, where this value for F-BF was almost 75%. The amount of braced bays is efficient parameter in reducing the base storey drifts.

Time history responses of base story drifts for S-BF and F-BF under *Kocaeli* earthquake are given in Fig. 8. According to the time history analysis S-BF and F-BF having SCs with the thickness of 18 and 25 mm showed good performance in reducing the base storey drifts throughout the whole duration of the earthquake. The average values of maximum storey drifts of bare and braced frames having SCs with varying thicknesses are illustrated in Fig. 9.

The results of analysis showed that thickness increment of SCs provides reduction not only in the base storey drifts but also in the upper story drifts. Braced frames having
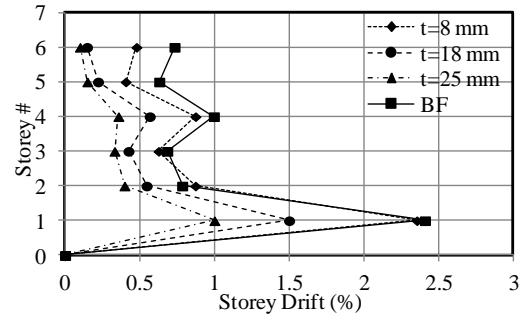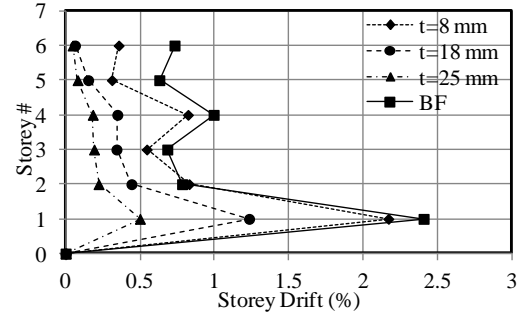
(a) Semi-Braced Frame (S-BF)
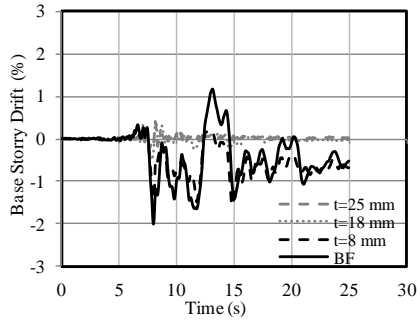
(b) Full Braced Frame (F-BF)

Fig. 8 Displacement time histories for S-BF and F-BF

(a) Semi-Braced Frame (S-BF)

(b) Full Braced Frame (F-BF)

Fig. 9 Storey drifts of bare and braced frames having SCs with varying thicknesses
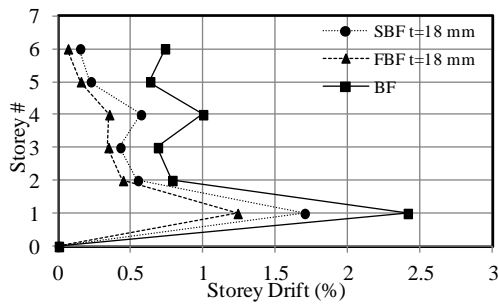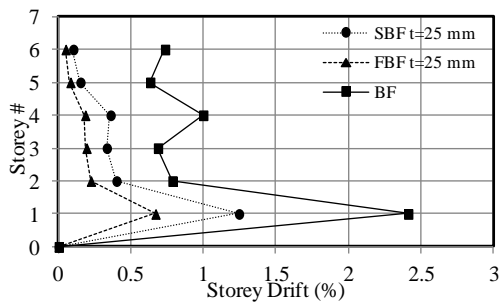

(a) *t*=18 mm

(b) *t*=25 mm

Fig. 10 Storey drifts of bare and braced frames having SCs with thickness of 18 and 25 mm

thicker SCs perform better in reducing storey drifts than that of the ones having thinner SCs. According to the average maximum storey drifts, S-BF and F-BF having SCs with the thickness of 25 mm could achieve to keep the frame 1.0% and 0.5% respectively drift levels which ensure the *immediate occupancy* (IO). Averages of the maximum drift levels of S-BF and F-BF having SCs with the thicknesses of 18 mm were 1.5% and 1.2% respectively

which indicates that both types of bracing system having 18 mm thick SCs could satisfy the *life safety* (LS) performance level. Average values for the maximum storey drifts of BF, S-BF and F-BF having SC with the thickness of 18 and 25 mm are separately given in Fig. 10 in order to evaluate the effect of the amount of braced bays. The upper storey drifts are similar in the case of S-BF and F-BF. It should be noted that the amount of braced bays is not effective to reduce upper storey drifts.

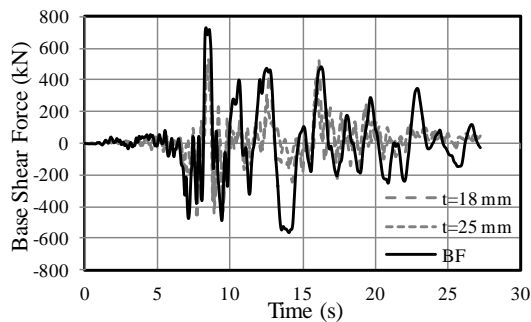### 3.2 Base storey and inter storey shear forces

Maximum base shear forces and base shear force reduction ratios for the frames having SCs with the thickness of 18 and 25 mm under the affect of 13 earthquake records are summarized in Table 8. Base shear reduction ratio is calculated as the ratio of maximum base shear force difference between bare and braced frame to the maximum base shear force of the bare frame.

Numerical simulation results showed that seismic base shear forces reduce for all the braced frame cases. The average base shear reduction ratios vary in the range of 25% to 31% and 26% to 27% for the F-BF and S-BF respectively. The reduction ratios are almost similar to each other for the case of different thicknesses of SCs. The probable reason for this small difference is that the increment of thickness of SCs results with an increment in global stiffness of the structure. Thus, the total base shear demand of the structure increases.
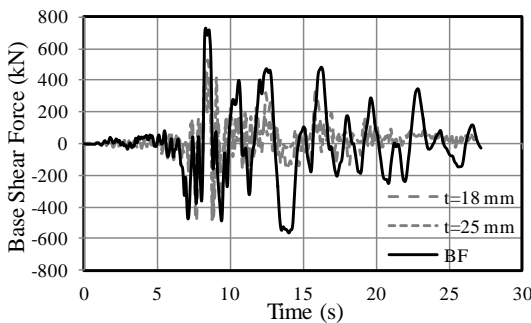
Time history responses of seismic base shear forces for bare and braced frames having SCs with the thickness of 18 mm under the affect *Kocaeli* earthquake are given in Fig. 11. Time history results show that both types of bracing

Table 8 Maximum base shear forces calculated for the bare and braced frames.

EQ	Bare Frame	Semi-Braced Frame (S-BF)		Full- Braced Frame (F-BF)		Reduction (%) S-BF		Reduction (%) F-BF	
		t:18 mm	*t*:25 mm	*t*:18 mm	*t*:25 mm	*t*:18 mm	*t*:25 mm	*t*:18 mm	*t*:25 mm
12011	689.9	516.3	537.7	540.25	529.58	25	22	22	23
12012	768.6	525.3	549.1	552.78	541.01	32	29	28	30
12041	782.4	556.9	543.7	556.58	548.56	29	31	29	30
12061	616.0	507.6	512.9	527.64	544.28	18	17	14	12
12072	728.0	502.8	526.7	545.02	534.75	31	28	25	27
12081	725.6	541.1	528.7	530.92	483.10	25	27	27	33
12091	668.2	536.9	544.4	518.91	501.071	20	19	22	25
12121	772.9	524.0	507.8	510.61	496.074	32	34	34	36
12122	845.0	500.2	512.9	524.28	526.31	41	40	38	38
12132	782.1	660.0	610.8	710.47	550.13	16	22	9	30
12141	639.8	472.8	475.6	480.02	260.93	26	26	25	60
12142	728.5	564.1	544.7	541.34	487.89	23	25	26	33
12151	687.2	560.2	536.8	537.56	542.30	19	22	22	21
Av.	*725.7*	*536.0*	*533.2*	*544.34*	*503.54*	*26*	*27*	*25*	*31*

(a) *t*=18 mm

(b) *t*=25 mm

Fig. 12 Storey shear forces of bare and braced frames having SCs with same thicknesses

(a) Semi-Braced Frame S-BF

(b) Full-Braced Frame F-BF

Fig. 11 Base shear time history responses for Kocaeli earthquake

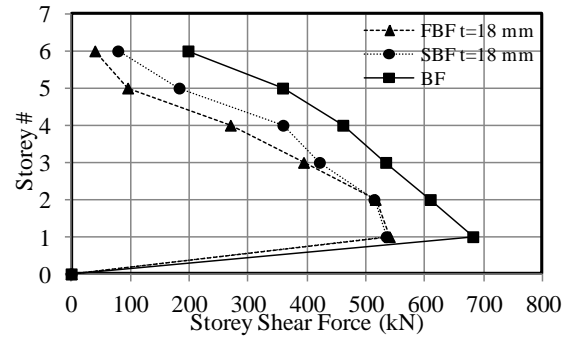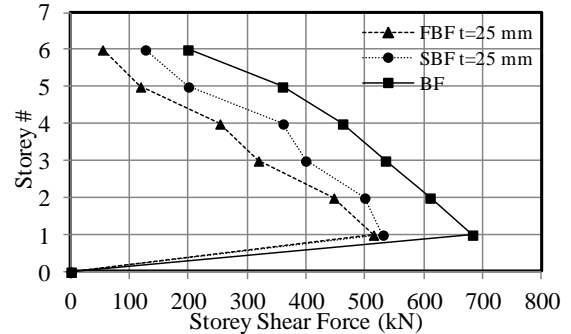system have sustainable performance in reducing the seismic base shear forces.

Average values of maximum storey shear forces for the bare and braced frames having SCs with the same thicknesses are illustrated in Fig. 12. It should be noted that in all cases of braced frames, 18 and 25 mm are appropriate thicknesses for SCs to reduce the average maximum storey shear forces when compared with the bare frame. Full braced frame has better performance in reducing the upper storey shear forces than that of the S-BF.

3.3 Energy dissipation

Seismic performance and the damage level of a structure mainly depend on the energy dissipation capacity of structural members. The seismic input energy (E_I) transformed to a structure, turns into mainly four components, Fig. 13. These components are the elastic strain (E_S), kinetic energy (E_K), damping energy (E_D) and plastic energies (E_{PSM}) dissipated by structural members, (Uang and Bertero 1990). Portion of EPSM could be
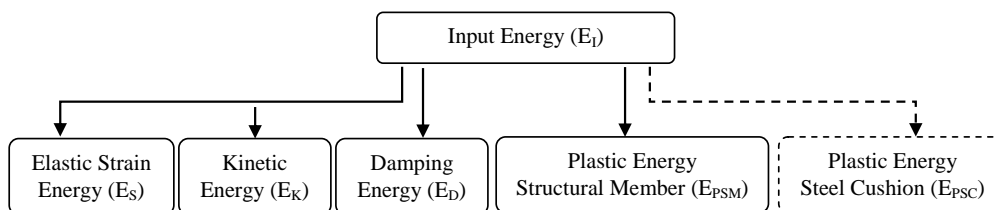

Fig.13 Energy components

Table 9 Plastic energy dissipated by the structural members (EPSM) at the base storey

| Base Storey Energy Dissipations (kNmm)	Bare Frame	Semi-Braced Frame				Full-Braced Frame			
		t=18 mm		t=25 mm		t=18 mm		t=25 mm	
EQ#	E_{PSM}	E_{PSM}	E_{PRR}	E_{PSM}	E_{PRR}	E_{PSM}	E_{PRR}	E_{PSM}	E_{PRR}
12011	165700	68686	59	73304	56	85892	48	6809	96
12041	208010	26580	87	40758	80	49937	76	11340	95
12012	205120	34676	83	26257	87	36626	82	18961	91
12061	264840	54211	80	35599	87	38848	85	8265	97
12072	138880	31550	77	44080	68	37965	73	8373	94
12081	123930	7549	94	4324	97	6766	95	3176	97
12091	202770	22567	89	11364	94	12053	94	3540	98
12121	207040	8080	96	8546	96	7785	96	4339	98
12122	221750	40300	82	29895	87	39559	82	22108	90
12132	198790	43532	78	43344	78	49838	75	17938	91
12141	106240	6817	94	2953	97	2048	98	630	99
12142	462990	18768	96	8026	98	8817	98	993	100
12151	185060	25012	86	8131	96	6040	97	5132	97
Average	*207009*	*29871*	*85*	*25891*	*86*	*29398*	*85*	*8585*	*96*

reduced by implementation of additional energy dissipater devices throughout the structure. The plastic energy dissipated by supplementary devices refers to the plastic energy dissipated by SCs (E_{PSC}) in this study.

Plastic energy dissipation of structural members (E_{PSM}) was determined by calculating the enclosed area of the total base shear forces subjected to column elements versus base storey displacement relations. Implementation of SCs throughout the structure could reduce the plastic energy demands of structural members. This reduction is quantified as per *plastic energy reduction ratio* (E_{PRR}), which is defined as the ratio of differences between E_{PSM} of bare and braced frame to E_{PSM} of the bare frame at the base storey, Eq. (6). Plastic energy values of structural members (E_{PSM}) and the reduction values (E_{PRR}) for bare and braced frames having SCs with the thickness of 18 and 25 mm are tabulated in Table 9.

$$E_{PRR}(\%) = \frac{E_{PSM_{Bare}}(\%) - E_{PSM_{Braced}}(\%)}{E_{PSM_{Bare}}(\%)} \times 100 \qquad (6)$$

It should be noted that at the base storey of the braced frames, the average plastic energy dissipation (E_{PSM}) is much less than that of the bare frame. The average values of E_{PRR} varying in between 85% to 96% which indicates that SCs with the thickness of 18 mm and 25 mm have considerable effects in reducing the plastic energy demands and damage propagation of structural members. The analysis results showed that the performance of F-BF having SCs with the thickness of 18 mm in reducing the plastic energy demand of structural members at the base storey is nearly same with the performance of S-BF.

Force-displacement relations of a SC used at the base storey having 18 mm thickness under the effect of *Kocaeli* earthquake record are given in Fig. 14. It is apparent that the displacement demand of SC with the thickness of 25 mm is less than that of the SC with the thickness of 18 mm.
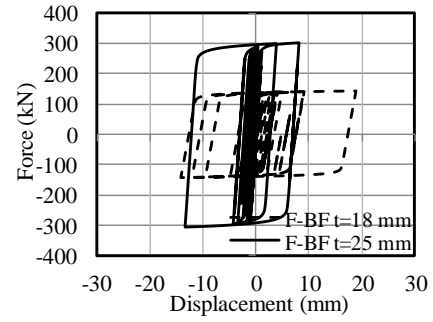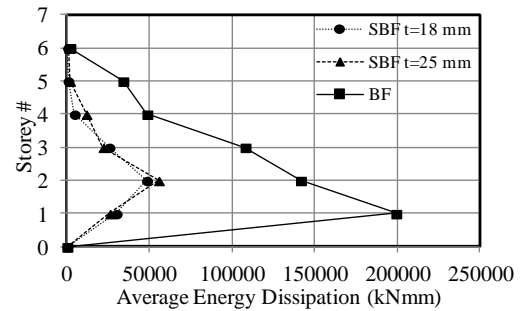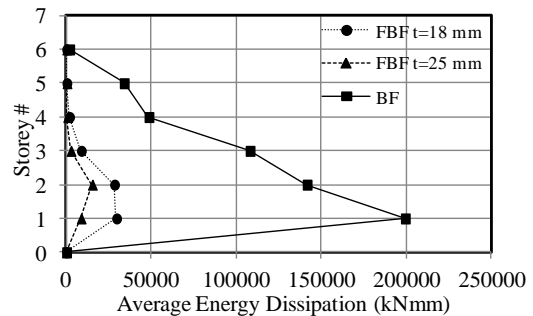

(a) Semi-Braced Frame (S-BF)
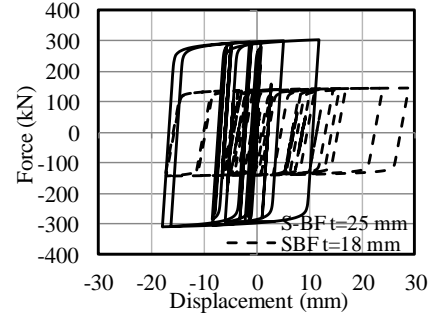
(b) Full-Braced Frame (F-BF)

Fig. 14 Force-displacement relations of link element model of SBF and FBF

(a) Semi-Braced Frame (S-BF)

(b) Full-Braced Frame (F-BF)

Fig. 15 Average plastic energy dissipation of braced frame for varying thickness

The force-displacement relations showed that SCs were able to dissipate plastic energy (E_{PSC}) during the analysis. Plastic energy reduction ratios (E_{PRR}) confirms that the plastic energy dissipated by structural members (E_{PSM}) reduces due to the fact that considerable amount of plastic energy was dissipated through SCs (E_{PSC}).

Average plastic energy dissipation of S-BF and F-BF
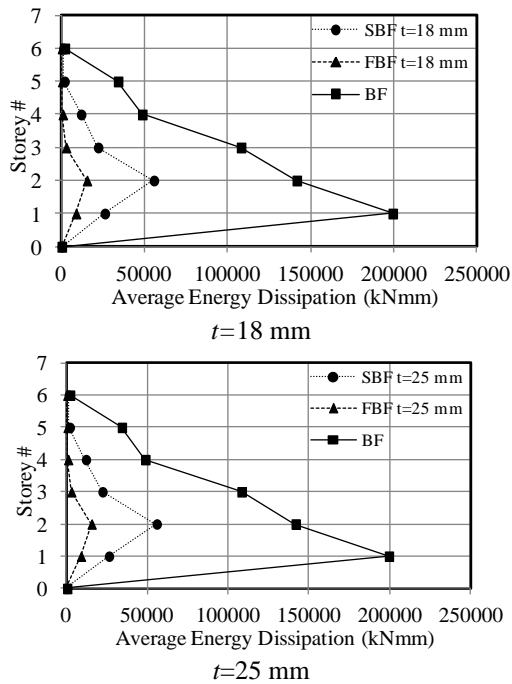
t=18 mm

t=25 mm

Fig. 16 Average plastic energy dissipation comparison of S-BF and F-BF

obtained at each storey for the SC thickness of 18 and 25 mm are given in Fig. 15 in comparison with the bare frames. Implementation of SCs to the structure can significantly decrease the plastic energy dissipation demands of primary structural members throughout the height of the structure. Increment of thickness of SCs reduces the average E_{PSM} values of F-BF, where almost no difference was observed in the case of S-BF.

The average E_{PSM} values for the bare and braced frames having SC thickness of 18 and 25 mm are given in Fig. 16. It should be noted that E_{PSM} values of bare and braced frames at the top storey are almost same. The main reason for this is the fact that the storey drift demands occurred at the top storey were minor. Consequently, SCs could not contribute energy dissipation and almost no reduction was observed in E_{PSM} values of the structural elements of top storey.

Seismic performance of F-BF and S-BF were almost similar to each other interms of energy dissipation in the case of 18 mm SC thickness throughout the height of the frame. However, F-BF having SC with the thickness of 25 mm have better performance than that of S-BF.

4. A brief optimization

In this part of the study, a brief optimization was performed on the aforementioned six-storey and four-bay RC building, in order to evaluate the effects of the damper configuration.

Although there are various studies in the literature about the metallic dampers, little attention has been paid for determining the effects of the quantity and arrangement of these dampers on the seismic responses of structures.

Ashour and Hanson (1987) proposed a method for optimum arrangement of dampers which could maximize the damping ratio of fundamental mode. Zhang and Soong (1992) proposed a sequential search algorithm in order to find the optimum location for viscoelastic dampers. Garcia (2001) suggested a simplified sequential search algorithm determining the best damper location and damper coefficient distribution in order to obtain the minimum interstorey velocities. Takewaki (2000) presented the optimal damper placement for a frame building using a minimum transfer function. This type of optimal damper design requires arrangement of the dampers to the storey where the interstorey drift values are the maximum. Aydın *et al*. (2006) studied the optimal damper placement based on transfer function of the base shear force for frame building with soft storey. Provided that the dampers are placed according to base shear force, the base shear force response of the structure decreases more effectively. This type of optimal damper design requires placing the dampers from the first storey to the upper stories in decreasing quantities. Aydın (2013) proposed to find optimal damper placement in shear buildings which minimize the cost under a target added damping ratio and interstorey drift ratio. Tovar and López (2004) stated in their study that, *"if one damper is placed, this should be located at the first story in order to obtain the best overall drift reduction. The best damper placement is one damper per story; if the number of dampers is less than the number of stories, one damper per story beginning at the lowest story is the best choice."* Structures require that the dampers should be placed at each storey in order to have a continuous vertical line of dampers (Whittaker *et al*. 1993). Optimum damper arrangement and the efficiency can be achieved by placing the devices at locations where the displacement or relative displacement is the largest. Metallic dampers and friction dampers are evaluated as displacement based devices and their force-deformation responses only depend on the relative displacement between each end of device. Friction dampers could be effective when they are placed close to regions of maximum inter-storey drift. They could be effective on energy dissipation only if slip displacement is reached, (Farsangi and Adnan 2012, Qu and Li 2012)

The current literature showed that the damper distribution significantly influences the structural seismic response. Moreover, most of the optimization studies in the literature that aim to determine the best damper arrangement basis on genetic algorithm methods; because the possible locations of the dampers used through the structure are numerous. However, in this part of the study, a brief optimization was applied on three groups of braced frames (BRFRs) which were selected according to the proposals derived from the literature. The first group of frames has SCs with different thicknesses and arrangement but equal quantity where, the second and the third group have SCs with different quantity and arrangement, (Figs. 17-19). The first braced frame of the first group (*BRFR1-1*) includes SCs with the thickness of 18 mm. The third braced frame of the first group is denoted as *BRFR1-3* having SCs with the thicknesses of 18 mm used at upper stories and having SCs with the thickness of 25 mm used at lower stories. The names of the frames were arranged as the first
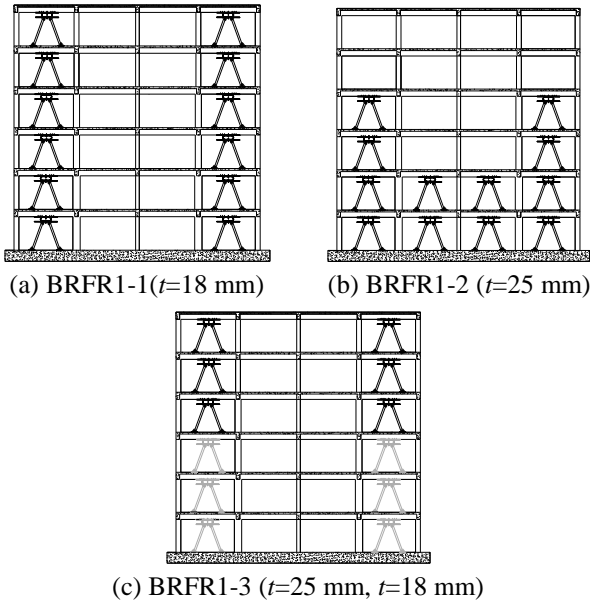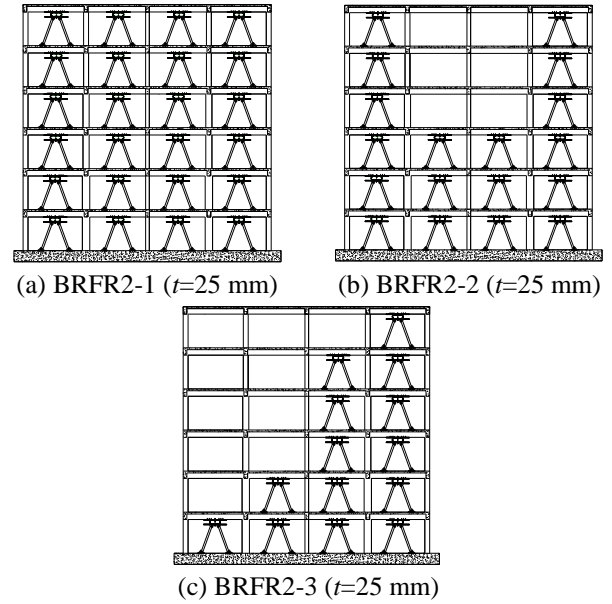
(a) BRFR1-1(*t*=18 mm)   (b) BRFR1-2 (*t*=25 mm)

(c) BRFR1-3 (*t*=25 mm, *t*=18 mm)

Fig. 17 First group SC configuration

(a) BRFR2-1 (*t*=25 mm)   (b) BRFR2-2 (*t*=25 mm)

(c) BRFR2-3 (*t*=25 mm)

Fig. 18 Second group SC configuration

(a) BRFR3-1 (*t*=25 mm)   (b) BRFR3-2 (*t*=25 mm)
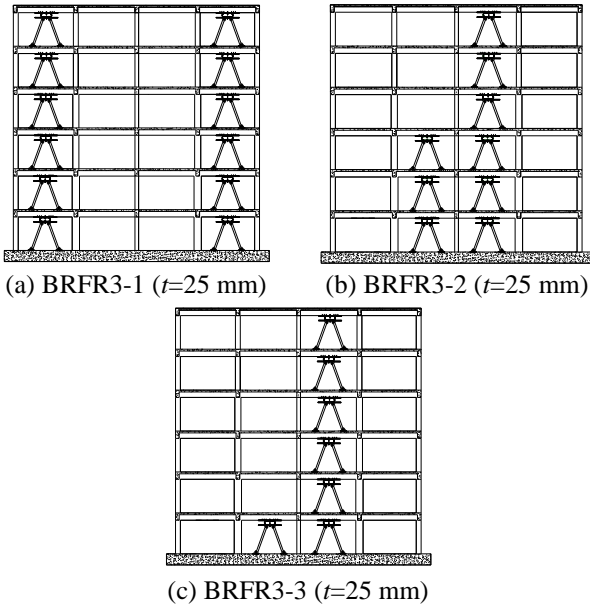

(c) BRFR3-3 (*t*=25 mm)
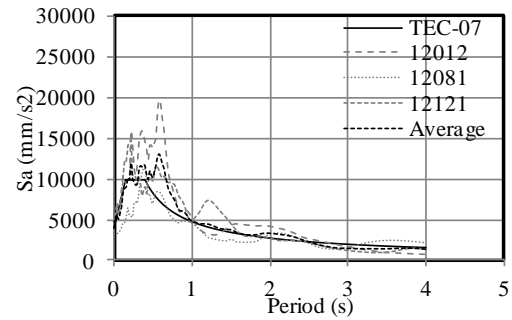
Fig. 19 Third group SC configuration

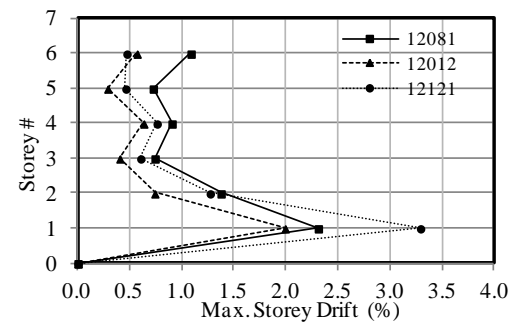Fig. 20 Spectrum curves of selected records

Fig. 21 Maximum storey drifts of the bare frame (*BF*)

number represents the number of the group and the second number shows the type of the braced frame.

Nonlinear time history analysis were performed on the braced frames by using three acceleration records selected from those of 13 far-field records given in Table 4. The names of the earthquake records are *Northridge* (*12012*), *Kocaeli* (*12081*) and *Superstition Hills* (*12121*). The acceleration spectra and the code-based spectrum are given in Fig. 20. All the modeling strategies for the nonlinear analytical model of the frame structure are same as explained in the related part of this study.

The optimum SC arrangement of each group was determined according to the obtained maximum storey drifts and compared with the performance levels of FEMA 356. The performance levels are illustrated in Table 7. The maximum storey drift values of the bare frame (*BF*)

obtained from nonlinear time history analysis are given in Fig. 21. The analysis results showed that bare frame (*BF*) could not achieve both *immediate occupancy* (*IO*) and *life safety* (*LS*) performance levels under the seismic excitations of 3 selected earthquakes.

The maximum storey drifts which belong to the first, second and the third groups are given in Figs. 22-24 respectively.

The analysis results showed that *BRFR1-2* reached to the *collapse prevention* (*CP*) level. The main reason for this behavior is that no SCs were used after the fourth storey of the frame structure. It should be noted that the SCs should
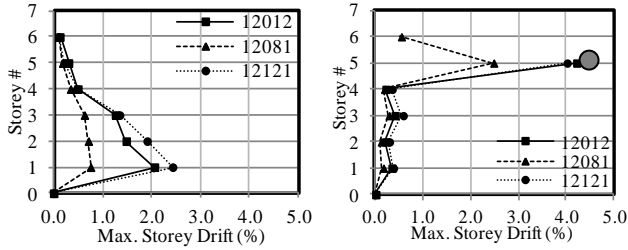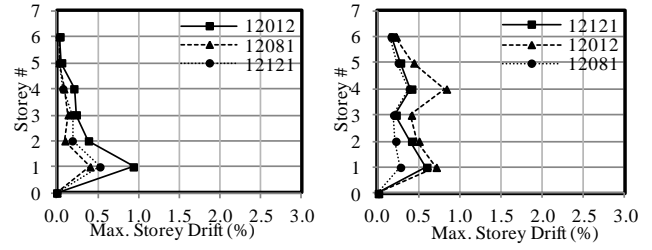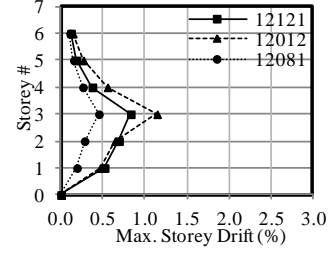
(a) BRFR1-1 (*t*=18 mm)

(b) BRFR1-2 (*t*=25 mm)
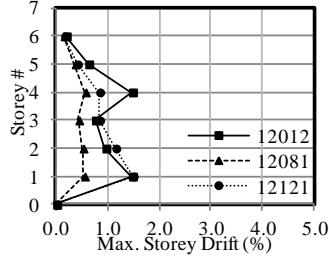
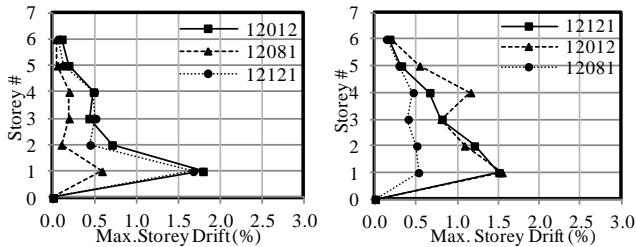(c)BRFR1-3 (*t*=25 mm, *t*=18 mm)

Fig. 22 First group performances

(a) BRFR2-1 (*t*=25 mm)
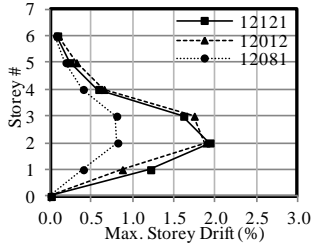

(b) BRFR2-2 (*t*=25 mm)

(c) BRFR2-3 (*t*=25 mm)

Fig. 23 Second group performances

(a) BRFR3-1 (*t*=25 mm)

(b) BRFR3-2 (*t*=25 mm)

(c) BRFR3-3 (*t*=25 mm)

Fig. 24 Third group performances

Table 10 Quantity of SCs and the maximum storey drifts

Frame ID	Number of used SCs	Max. Storey Drift (%)	Performance Levels
BRFR1-1	12	2.5	Collapse Prevention (CP)
BRFR1-2	12	5.7	Collapse Prevention (CP)
BRFR1-3	12	1.5	Life Safety (LS)
BRFR2-1	24	1.0	Immediate Occupancy (IO)
BRFR2-2	18	0.8	Immediate Occupancy (IO)
BRFR2-3	14	1.1	Immediate Occupancy (IO)
BRFR3-1	12	1.7	Life Safety (LS)
BRFR3-2	9	1.5	Life Safety (LS)
BRFR3-3	7	1.9	Life Safety (LS)

be arranged continuously throughout the height of the structure. The maximum storey drift values showed that *BRFR1-1* exceeded the performance level of *life safety* (*LS*), where *BRFR1-3* achieved to stay within this performance level. The increment of the thickness of SCs placed at lower stories where the relative displacement demands were high; is an efficient application to increase the seismic performance of the frame. *BRFR1-3* could be evaluated as the best damper arrangement among the first group members.

The results derived from nonlinear time history analysis of the second group frames showed that, all the braced frames (*BRFR 2-1, 2-2* and *2-3*) could satisfy the *immediate occupancy* (*IO*) performance level. It should be noted that using numerous SCs is not always the best damper arrangement for the frame. Target performance level of *immediate occupancy* (*IO*) could also be satisfied by using

relatively less quantity of SCs. The placement of SCs starting from the first storey to the upper stories in decreasing quantities is an optimal SC arrangement.

According to the third group analysis results, all the members of the group could achieve the *life safety* performance level (*LS*). If one may prefer to use minimum quantity of SC, *BRFR3-3* is an appropriate SC arrangement which satisfies the *life safety (LS)* level. *BRFR3-2* resulted with the maximum storey drift of 1.5% where the maximum drift of *BRFR3-3* was 2.0%. The seismic performance of the braced frames could be increased by adding SCs at lower stories. The increment of the number of SCs used at lower stories where the relative displacements are the largest increases the overall structural performance.

Maximum storey drift values obtained from the nonlinear time history analysis of 9 different bracing configurations and the quantity of SCs for each case are tabulated in Table 10. Performance level of *life safety* (*LS*) could be achieved by any configuration type of the third group frames. On the other hand, the performance level of *immediate occupancy* (*IO*) could be satisfied by any

configuration types of the second group frames. Application of full bracing (F-BF) which corresponds to the case of *BRFR2-1* is not compulsory to obtain the *immediate occupancy* (*IO*) performance level. The same performance level could be achieved by *BRFR2-3* option that includes only a bit more SCs than the *BRFR3-1*. Among 9 cases of braced frames *BRFR2-3* could be proposed as the optimum damper arrangement which achieves *immediate occupancy* (*IO*) performance level with the minimum quantity of SCs.

5. Conclusions

Nonlinear dynamic analyses were conducted to evaluate the effects of SCs on the global seismic behavior of a typical RC structure and the results are given below;

• Implementation of SCs is an efficient method in reducing the average maximum base storey drift values when compared with the bare frame. Thickness of SCs is effective variable to reduce the base storey and upper storey drifts. Amount of braced bays is effective in reducing base storey drift. However, amount of braced bays is not effective in reducing the upper storey drifts.

• Braced frames having SCs with the thickness of 25 mm could able to keep the frame within the *immediate occupancy* (IO) performance level, where S-BF and F-BF having SCs with the thicknesses of 18 mm could achieve the *life safety* (LS) performance level. Steel cushions with the thickness of 8 mm were not successful to improve the seismic performance of the frame.

• Implementation of SCs with the thickness of 18 and 25 mm to a typical six storey RC frame reduces the seismic base shear forces in all cases. Performance of braced frames having SCs with the thickness of 18 and 25 mm are almost similar interms of base shear force reduction ratios. The main reason for this similarity is that the increments of thickness of SCs also increase the global stiffness and force demand of the RC frame.

• The average plastic energy dissipated at the base storey of the braced frames is much less than that of the bare frame. The energy dissipation demand on primary structural members throughout the structure was considerably reduced, along with the potential for structural damage.

• Braced frames having SCs with the thickness of 18 mm behaved almost similar interms of energy dissipation. However, F-BF having SC with the thickness of 25 mm have better performance than that of S-BF in reducing EPSM values.

• The contribution of SCs interms of energy dissipation at the top storey is almost negligible. The main reason for this result is the fact that the inter-story drifts were minor at the top stories.

• The optimization study resulted that the SCs should be arranged continuously through the height of the structure. Implementation of numerous SCs to the frame structure is not always the optimum alternative. The target performance level could also be achieved by using relatively less quantity of SCs. Among the 9 configuration cases, *BRFR2-3* could satisfy the

immediate occupancy (*IO*) performance level with the minimum number of SCs. Increment of the number of SCs used at lower stories is effective to increase the overall structural performance.

• The nonlinear time history analyses were performed on a limited number of SC configuration cases and some important results were derived. Although these results are valid within the selected group of braced frames, there is a need for further extensive optimization studies which takes account a wide range of alternatives. Accordingly, determination of the best damper configuration and design of SCs are among the future research subjects of the author.

References

Alehashem, S.M.S., Keyhani, A. and Pourmohammad, H. (2008), "Behavior and performance of structures equipped with adas & tadas dampers", *Proceedings of the 14th World Conference on Earthquake Engineering*, Beijing, China, October.

Ashour, S. and Hanson, R. (1987), "Elastic response of buildings with supplemental damping", Rep. No. UMCE 87-1 1987, Dept. of Civ. Engrg. Univ. of Michigan, Ann Arbor, Michigan, USA.

Aydin, E. (2013), "A simple damper optimization algorithm for both target added damping ratio and interstorey drift ratio", *Earthq. Struct.*, **5**(1), 83-109.

Aydin, E., Boduroglu, M.H. and Guney, D. (2006), "Optimal damper distribution for seismic rehabilitation of planar building structures", *Eng. Struct.*, **29**, 176-185.

Bergman, D.M. and Gool, S.C. (1987), "Evaluation of cyclic testing of steel-plate devices for added damping and stiffness", Rep. No. UMCE 87-10, Univ. of Michigan, Ann Arbor, Michigan, USA.

Black, C.J., Makris, N. and Aiken, I. (2004), "Component testing seismic evaluation and characterization of buckling-restrained braces", *J. Struct. Eng.*, ASCE, **130**(6), 880-894.

Chan, R., Albermani, F. and Williams, M. (2009), "Evaluation of yielding shear panel device for passive energy dissipation", *J. Constr. Steel Res.*, **65**(2), 260-268.

Farsangi, E.N. and Adnan, A., (2012), "Seismic performance evaluation of various passive damping systems in high and medium-rise buildings with hybrid structural system", *Gazi Univ. J. Sci.*, **25**(3), 721-735.

FEMA 356 (2000), Prestandard and commentary for the seismic rehabilitation of buildings, Federal Emergency Management Agency, Washington, D.C.

FEMA 461 (2007), Interim testing protocols for determining the seismic performance characteristics of structural and nonstructural components, Federal Emergency Management Agency, Washington.

FEMAP695 (2009), Recommended methodology for quantification of building system performance and response parameters, Federal Emergency Management Agency, Redwood City, California.

Garcia, D.L. (2001), "A Simple method for the design of optimal

damper configurations in mdof sructures", *Earthq. Spectra*, **17**(3), 387-398.

Gray, M.G., Christopoulos, C. and Packer, J.A. (2010), "Cast steel yielding fuse for concentrically braced frames", *Proceedings of the 9th U.S National and 10th Canadian Conference on Earthquake Engineering*, Toronto, Canada, July.

Karalis, A.A., Georgiadi-Stefanidi, K.A., Salonikios, T.N., Stylianidis, K.C. and Mistakidis, E.S. (2011), "Experimental and numerical study of the behavior of high dissipation metallic devices for the strengthening of existing structures", *Compdyn 2011 III Eccomas Thematic Conference on Computational Methods in Structural Dynamics and Earthquake Engineering*, Corfu, Greece, May.

Kelly, J.M., Skinner, R.I. and Heine, A.J. (1972), "Mechanisms of energy absorption in special devices for use in earthquake resistant structures", *Bull. N.Z. Soc. Earthq. Eng.*, **5**(3), 63-87.

Maleki, S. and Bagheri, S. (2010), "Pipe damper, part I experimental and analytical study", *J. Constr. Steel Res.*, **66**(8-9), 1088-1095.

Mander, J.B., Priestley, M.J.N. and Park, R. (1988), "Theoretical stress-strain model for confined concrete", *J. Struct. Eng.*, **114**(8), 1804-1826.

Mazzolani, F.M. (2007), "Innovative metal systems for seismic upgrading of RC structures", *J. Constr. Steel Res.*, **64** (7-8), 882-895.

Oh, S.H., Kim, Y.J. and Ryu, H.S. (2009), "Seismic performance of steel structures with slit dampers", *Eng. Struct.*, **31**(9), 1997-2008.

Özkaynak, H., Güllü, A., Gökçe, T., Khajehdeh, A., Mahdavi, M., Azizisales, F., Bal, İ.E., Smyrou, E., Yüksel, E. and Karadoğan, H.F. (2014), "Energy dissipative steel cushions", *2nd European Conference on Earthquake Engineering and Seismology*, Istanbul, Turkey, August.

Priestley, M.J.N. (1991), "Overview of PRESSS research program", *J. Precast Concrete Inst.*, **36**(4), 50-57.

Qu, J. and Li, H. (2012), "Optimal placement of passive energy dissipation devices by genetic algorithms", *Math. Probl. Eng.*, **2012**(474282), 1-20.

Rai, D.C., Annam, P.K. and Pradhan, T. (2013), "Seismic testing of steel braced frames with aluminum shear yielding dampers", *Eng. Struct.*, **46**(2013), 737-747.

SafeCladding EU Project (2012-2015). "Improved fastening systems of cladding panels for precast buildings in seismic zones", Project FP7-314122, Research for SMEs Associations.

Sahoo, D.R. and Rai, D.C. (2010), "Seismic strengthening of non-ductile reinforced concrete frames using aluminum shear links as energy-dissipation devices", *Eng. Struct.*, **32**, 3548-3557.

Seismosoft (2014) "SeismoStruct v7.0 - A computer program for static and dynamic nonlinear analysis of framed structures", Available from http://www.seismosoft.com.

Shultz, A.E. and Magana, R.A. (1996), "Seismic behavior of connections in precast concrete walls", *Proceedings of Mete A. Sozen Symposium*, ACI SP 162, Farmington Hills, Michigan, August.

Takewaki, I. (2000), "Optimal damper placement for critical excitation", *Probab. Eng. Mech.*, **15**, 317-325.

TEC (2007), Specification for buildings to be built in seismic zones, Turkish Earthquake Design Code (2007), Ankara, Turkey.

Tovar, C. and López, O. (2004), "Effect of the position and number of dampers on the seismic response of frame structures", *Proceedings of the 13th World Conference on Earthquake Engineering*, Vancouver, B.C., Canada, August.

Tsai, K.C., Chen, H.W., Hong, C.P. and Su Y.F. (1993), "Design of steel triangular plate energy absorbers for seismic resistant construction", *Earthq. Spectra*, **19**(3), 505-528.

TSE 498 (1997), Design loads for buildings, Turkish Standard Code 498, Ankara, Turkey.

Uang, C.M. and Bertero, V.V. (1990), "Evaluation of seismic energy in structures", *Earthq. Eng. Struct. Dyn.*, **19**(1), 77-90.

Valente, M. (2013), "Seismic protection of r/c structures by a new dissipative bracing system", *The 2nd International Conference on Rehabilitation and Maintenance in Civil Engineering Procedia Engineering*, **54**, 785-794.

Whittaker, A., Bergman, D., Clark, P., Cohen, S., Kelley, J. and Scholl, R. (1993). "1993 code requirements for design and implementation of passive energy dissipation systems", *The Energy Dissipation Working Group of the Base Isolation Subcommittee of the Structural Engineers Association of Northern California*, ATC-17-1, San Francisco, March.

Zhang, C., Zhou, Y., Weng, D.G, Lu, D.H. and Wu, C.X. (2015), "A methodology for design of metallic dampers in retrofit of earthquake-damaged frame", *Struct. Eng. Mech.*, **56**(4), 569-588

Zhang, R. and Soong, T. (1992), "Seismic design of viscoelastics dampers for structural applications", *J. Struct. Eng.*, **118**(5), 1375-1392.

CC